

Traffic reconstruction using autonomous vehicles

Maria Laura Delle Monache, Thibault Liard, Benedetto Piccoli, Raphael E. Stern, Daniel B. Work

▶ **To cite this version:**

Maria Laura Delle Monache, Thibault Liard, Benedetto Piccoli, Raphael E. Stern, Daniel B. Work. Traffic reconstruction using autonomous vehicles. SIAM Journal on Applied Mathematics, 2019, 75 (5), pp.1748-1767. 10.1137/18M1217000 . hal-01882309

HAL Id: hal-01882309
https://inria.hal.science/hal-01882309

Submitted on 26 Sep 2018

HAL is a multi-disciplinary open access archive for the deposit and dissemination of scientific research documents, whether they are published or not. The documents may come from teaching and research institutions in France or abroad, or from public or private research centers.

L'archive ouverte pluridisciplinaire **HAL**, est destinée au dépôt et à la diffusion de documents scientifiques de niveau recherche, publiés ou non, émanant des établissements d'enseignement et de recherche français ou étrangers, des laboratoires publics ou privés.

Traffic reconstruction using autonomous vehicles

Maria Laura Delle Monache,* Thibault Liard†
Benedetto Piccoli‡ Raphael Stern§ Dan Work¶

Abstract

We consider a partial differential equation - ordinary differential equation system to describe the dynamics of traffic flow with autonomous vehicles. In the model the bulk flow is represented by a scalar conservation law, while each autonomous vehicle is described by a car following model. The autonomous vehicles act as tracer vehicles in the flow and collect measurements along their trajectory to estimate the bulk flow. The main result is to prove theoretically and show numerically how to reconstruct the correct traffic density using only the measurements from the autonomous vehicles.

Keywords: Scalar conservation laws, PDE-ODE systems, Density reconstruction, Traffic flow models

AMS classification: 35L65; 90B20

1 Introduction

In recent years Autonomous Vehicles (briefly AVs) have been tested on urban and highway networks and appear to be the technology with the highest chance of disruptive changes for the future of traffic monitoring and management. Traffic monitoring already underwent a major disruption when the use of fixed location sensor and cameras has been supplemented by Lagrangian sensing via mobile phones and other devices. AVs will further contribute by acting as highly reliable moving sensors being equipped with high-tech on-board devices. The aim of this paper is to show how a small number of AVs immersed in bulk traffic is capable of monitoring the traffic density along a road without any other data source. Mathematically we rely on a coupled ODE-PDE model representing the combined evolution of bulk traffic density and AVs positions.

*Univ. Grenoble Alpes, Inria, CNRS, Grenoble INP, GIPSA-Lab, 38000 Grenoble, France (email: ml.dellemonache@inria.fr).

†Univ. Grenoble Alpes, Inria, CNRS, Grenoble INP, GIPSA-Lab, 38000 Grenoble, France (email: thibault.liard@inria.fr).

‡Rutgers University-Camden, NJ, USA (email: piccoli@camden.rutgers.edu).

§Vanderbilt University, TN, USA (email: stern5@illinois.edu).

¶Vanderbilt University, TN, USA (email: dan.work@vanderbilt.edu).

Let us start providing some background on traffic estimation. The field of traffic reconstruction began with experiments in the Lincoln Tunnel in New York City [14, 25], which since then have seen significant development in terms of the modeling as well as the estimation algorithms [26, 27, 18]. For a recent summary of the developments of model based traffic estimation, see [20, 11]. More recently there has been interest to explore estimation in the Lagrangian coordinates [28, 15] where sensors are embedded in the traffic flow instead of being placed at fixed locations in the infrastructure. For example, the *Mobile Century* project [16, 27] used GPS data from mobile phones as measurements for Lagrangian traffic state estimation. Such Lagrangian traffic state estimation techniques have often relied on GPS data from the vehicles [27, 13], and more recently spacing measurements from sensors on the vehicle [21]. Recognizing AVs are also highly instrumented vehicles, and may be able to provide additional measurements that can improve traffic estimation.

We now turn gears toward the mathematical aspects of the paper. One of the most used macroscopic model in traffic is the celebrated Lighthill-Whitham-Richards model [17, 19], which consists of a single conservation law for the traffic density. Particle trajectories for such model represent car trajectories and can be reconstructed using solutions to discontinuous Ordinary Differential Equations (ODEs) see [6]. Considering together the traffic density and a small number of particle trajectories gives rise to a partially coupled PDE-ODE system, where the ODEs depend on the PDE solution but not vice versa [5]. In [8] the authors introduced a model for with moving flux constraints. The latter represent a moving bottleneck, which in turn may correspond to a large truck or bus as well as an AV driving differently than the bulk traffic. Such model is a completely coupled PDE-ODE model. Here we assume that the AVs do not influence traffic by their driving thus we resort to the partially coupled model.

Our problems can be formulated as a control ones. We consider a stretch of road with incoming and outgoing traffic and a small number of AVs entering the road and measuring the density at their location. The aim is to control the AV speed (compatibly with the traffic conditions) in such a way that the collected data allows a complete reconstruction of the traffic density along the road after a certain time. This corresponds to generate moving boundaries, by controlling the AVs, so that the solution to the conservation law compatible with measure data along such boundaries is unique. Such problem is, to our knowledge, new and can be addressed using typical tools from the theory of conservation laws. More specifically, initial-boundary value problems are well understood [10, 2, 22, 23] and semigroup of solutions are constructed via wave-front tracking [9, 1, 3]. Using these results, we first show that it is possible to define explicitly a time horizon such that, if such horizon is finite, then complete traffic reconstruction is possible for all times after such horizon. Moreover, the main result (Theorem 1) determines all initial conditions which give rise to the observed density at the time horizon. The result is then extended to the case of a ring road.

We then turn to the attention to the problem of reconstructing the density from the AVs measurement (which was proved possible by the main Theorem 1).

Again using wave-front tracking approach, we define an algorithm with input the AVs data and output the reconstructed traffic density. Since we use wave-front tracking, our solution is piecewise constant in time-space, the AVs trajectories present piecewise constant speed, changing only at the times when the AV meet a wave. Therefore, all data, including AVs trajectories and measurement, are finite dimensional and the algorithm can be implemented on a regular personal computer. We are then able to present various numerical experiments of traffic reconstruction along a stretch of road.

The paper is organized as follows. In Section 2, we briefly introduce the coupled ODE PDE model before describing the main theoretical results in Section 3. In Section 4 a numerical scheme to estimate the traffic density from the AVs is introduced, and in Section 5 the scheme is applied to numerical experiments. Section 6 discusses possible extensions of the work.

2 Model description

By detecting local density via sensors of autonomous vehicles, we want to reconstruct the density at a certain time T and on a portion of a road. In order to do this, we need to be able to describe the traffic dynamics and reconstruct the density starting from the measurement of the autonomous vehicles.
Let us consider a stretch of road $\mathbb{R}$ with mixed traffic, i.e., partly human-piloted traffic and partly autonomous vehicles. This situation can be modeled with a PDE-ODEs system consisting of a scalar conservation law accounting for the human-piloted traffic and a system of ODEs describing the dynamics of the autonomous vehicles. From a mathematical point of view this means that the main bulk of human-piloted traffic is described with the *Lighthill-Whitham-Richards* (LWR) macroscopic model, [17, 19], i.e. the mass conservation equation

$$\partial_t \rho + \partial_x f(\rho) = 0 \qquad (t, x) \in \mathbb{R}^+ \times \mathbb{R} \tag{1}$$

where $\rho = \rho(t, x) \in [0, \rho_{\max}]$ is the mean traffic density, $\rho_{\max}$ is the maximal density and the flux function $f : [0, \rho_{\max}] \to \mathbb{R}^+$ is given by the following flux-density relation:

$$f(\rho) = \rho v(\rho), \tag{2}$$

where $v(\rho)$ is a smooth decreasing function denoting the mean traffic speed. We will assume for simplicity that the following hold:

(A1) $\rho_{\max} = 1$;

(A2) $f(0) = f(1) = 0$;

(A3) f is a strictly concave function.

Assumptions (A2), (A3) ensure the uniqueness of a maximum point of the flux function at a density $\rho_{\text{cr}} \in [0, 1]$.
A typical example of flux function for the LWR model is given in Figure 1.

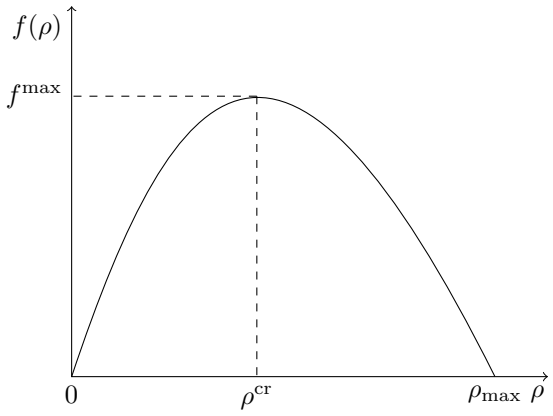


Figure 1: Flux function of equation (1), commonly referred to as fundamental diagram in the transportation literature.

We consider that along the road at a certain time t there are N autonomous vehicles that are able to detect local density via sensors. We assume that we can collect their information starting at a position $x = \alpha \in \mathbb{R}$ and at time $t \geqslant 0$. The N autonomous vehicles are distributed in two groups N_1, $N_2 + 1$ in the following way (see Figure 2):

- N_1 vehicles enter the stretch of road considered at time $t > 0$ at $x = \alpha$.
- $N_2 + 1$ vehicles are located at time $t = 0$ in a position $x \geqslant \alpha$.

All the autonomous vehicles are modeled via the following ODE-system

$$\begin{cases} \dot{y}_i(t) = u_i(\rho(t, y_i(t)+)) & t \in [t_i, +\infty], i = -N_1, \cdots, N_2, \\ y(t_i) = y_0^i & i = -N_1, \cdots, N_2. \end{cases} \tag{3}$$

Above, u_i is a decreasing function verifying that

$$\begin{cases} u_i(\rho) > f'(\rho) & \text{if } \rho > 0, \\ u_i(\rho) = f'(\rho) & \text{if } \rho = 0. \end{cases} \tag{4}$$

If $i \in \{-N_1, \cdots, -1\}$, the vehicles enter the road $[\alpha, \infty)$ at time $t_i > 0$ in a position $y_0^i = \alpha$. If $i \in \{0, \cdots, N_2\}$, the vehicles are already in the stretch of road $[\alpha, \infty)$, therefore $t_i = 0$ and $\alpha \leqslant y_0^i$.

The Cauchy problem that describes the traffic dynamics is then:

$$\begin{cases} \partial_t \rho + \partial_x(f(\rho)) = 0, & (t, x) \in \mathbb{R}^+ \times \mathbb{R}, \\ \rho(0, x) = \rho_0(x), & x \in \mathbb{R}, \\ \dot{y}_i(t) = u_i(\rho(t, y_i(t)+))), & t > t_i, i = -N_1, \cdots, N_2 \\ y_i(t_i) = y_0^i, & i = -N_1, \cdots, -1 \end{cases} \tag{LWR-AVs}$$

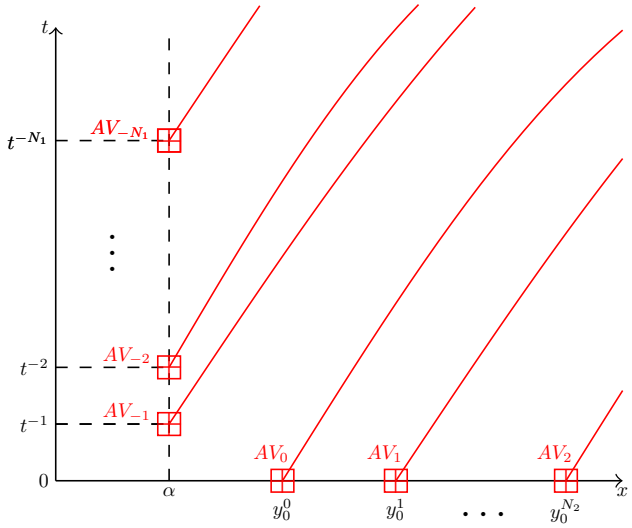


Figure 2: AVs along the road at a certain time t.

with

$$\begin{cases} t_{-N_1} > \cdots > t_{-1} > 0 = t_0 = \cdots = t_{N_2}, \\ y_0^{-N_1} = \cdots = y_0^{-1} = \alpha \leqslant y_0^0 < \cdots < y_0^{N_2}. \end{cases}$$

Above, $\rho_0(\cdot)$, and $y_0^i(\cdot)$ are the initial conditions. Our goal is to find a time T at which it is possible to reconstruct the true density ρ between two autonomous vehicles that depends only on the measured local density of each AV.

3 Main results

Let us first introduce the following operators that aim at simplifying the notation of the proofs:

- $S_t : L^1(\mathbb{R}) \cap BV(\mathbb{R}, [0,1]) \mapsto L^1(\mathbb{R}) \cap BV(\mathbb{R}, [0,1])$ is a L^1-Lipschitz semi-group defined by $S_t(\rho_0) = \rho(t, \cdot)$ s.t. ρ the solution of

$$\begin{cases} \partial_t \rho + \partial_x(f(\rho)) = 0, & (t,x) \in \mathbb{R}^+ \times \mathbb{R}, \\ \rho(0,x) = \rho_0(x), & x \in \mathbb{R}, \end{cases} \tag{LWR}$$

- $\Gamma : BV(\mathbb{R}, [0,1]) \cap L^1(\mathbb{R}) \to (C^0(\mathbb{R}_+, BV(\mathbb{R}, [0,1]) \cap L^1(\mathbb{R}))^2)^N$ defined by $\Gamma(\rho_0) = (\rho(\cdot, y_i(\cdot)\pm))_{i \in \{-N_1, \cdots, N_2\}}$ where (ρ, y_i) is the solution of (LWR-AVs) with initial data ρ_0. $\Gamma_i(\cdot)$ denotes the i^{th} component of $\Gamma(\cdot)$.

Let an unknown initial data $\bar{\rho}_0 \in BV(\mathbb{R},[0,1]) \cap L^1(\mathbb{R})$. For $i \in \{-N_1, \cdots, N_2 - 1\}$, by collecting only $(\Gamma_i(\bar{\rho}_0), \Gamma_{i+1}(\bar{\rho}_0)) := (\rho(\cdot, y_i(\cdot)\pm), \rho(\cdot, y_{i+1}(\cdot)\pm))$ via sensors of the i^{th} autonomous vehicle and the $(i+1)^{\text{th}}$ autonomous vehicle, we want to reconstruct $S_{T_i}(\bar{\rho}_0)(x)$ for every $x \in [y_i(T_i), y_{i+1}(T_i)]$ at a certain time $T_i \geqslant 0$. For every $i \in \{-N_1, \cdots, N_2\}$ the trajectory of the i-th autonomous vehicle is described by (3).

Example 1 shows that we cannot reconstruct the solution at any time. Theorem 1 gives a way to find the reconstruction time T.

Example 1. *Assuming that $f(\rho) = \rho(1-\rho)$ and one autonomous vehicle is deployed at $(0,0)$. Let $\rho_0 < \rho_1 < \rho_2$ and $\frac{1}{\rho_1} = \frac{1}{\rho_2 - \rho_0}$. We have $\Gamma(\tilde{\rho}_0) = \Gamma(\bar{\rho}_0)$ with $\tilde{\rho}_0 = \rho_0 \mathbb{1}_{(-\infty,1)} + \rho_1 \mathbb{1}_{(1,2)} + \rho_0 \mathbb{1}_{(2,\infty)}$, $\bar{\rho}_0 = \rho_0 \mathbb{1}_{(-\infty, 1+\frac{\rho_2-\rho_1}{\rho_2-\rho_0})} + \rho_2 \mathbb{1}_{(1+\frac{\rho_2-\rho_1}{\rho_2-\rho_0}, \infty)}$. Thus, for every $t \in [0, \frac{1}{\rho_2-\rho_1}]$, $S_t(\tilde{\rho}_0) \neq S_t(\bar{\rho}_0)$.*

We introduce $\varphi_i : \mathbb{R}_+^* \mapsto \mathcal{P}(\mathbb{R})$ defined by

$$\varphi_i(t) = [f'(\rho(t, y_i(t)-))(t_{i+1} - t) + y_i(t), f'(\rho(t, y_i(t)+))(t_{i+1} - t) + y_i(t)]. \quad (5)$$

Theorem 1. *Let $\bar{\rho}_0 \in BV(\mathbb{R},[0,1]) \cap L^1(\mathbb{R})$. For every $i \in \{-N_1, \cdots, N_2 - 1\}$, the i^{th} autonomous vehicle starts at time t_i in the position y_0^i and its trajectory is described by (3). Moreover, we impose that u_i verifies (4). Let $T_i \in \mathbb{R} \cup \{\infty\}$ defined by*

$$T_i := \sup_{\{T \in \mathbb{R}_+ \setminus y_0^{i+1} \in \varphi_i(T)\}} T. \quad (6)$$

If $T_i < \infty$ then for every $\rho_0 \in \Gamma^{-1}(\Gamma(\bar{\rho}_0))$, $S_{T_i}(\rho_0)(x) = S_{T_i}(\bar{\rho}_0)(x)$, for every $i \in \{-N_1, \cdots, N_2\}$ and for almost every $x \in [y_i(T_i), y_{i+1}(T_i)]$ with (y_i, y_{i+1}) solution of (3).

Example 2. *Assuming that $f(\rho) = \rho(1-\rho)$, $u_1(\rho) = 1 - \rho$ and two autonomous vehicles are deployed on the road at $(0, y_0^1)$ and at $(0, y_0^2)$. If we observe $\rho(t, y_1(t)) = \rho_1$ for every $t \in \mathbb{R}$, then $T_1 = \frac{y_0^2 - y_0^1}{u_1(\rho_1) - f'(\rho_1)}$ verifies (6).*

In Example 2, $\lim_{\rho_1 \to 0} T_1 = \lim_{\rho_1 \to 0} \frac{y_0^2 - y_0^1}{u_1(\rho_1) - f'(\rho_1)} = \infty$. Theorem 2 gives a sufficient condition on the initial density $\bar{\rho}_0$ to have a finite reconstruction time T.

Theorem 2. *We assume that, for every $x \in \mathbb{R}$, $0 < \rho_{\min} \leqslant \bar{\rho}_0(x) \leqslant \rho_{\max}$ and $c_i = \min_{\rho \in [\rho_{\min}, \rho_{\max}]} (u_i(\rho) - f'(\rho)) > 0$. We have, for every $i \in \{-N_1, \cdots, N_2\}$,*

$$\frac{y_0^{i+1} - y_0^i}{u_i(\rho_{\min}) - f'(\rho_{\max})} + t_{i+1} \leqslant T_i \leqslant \frac{(y_0^{i+1} - y_0^i + f'(\rho_{\min})(t_i - t_{i+1}))}{c_i} \left(1 + \exp\left(\frac{\alpha T V(\rho_0)}{c_i}\right)\right) \quad (7)$$

with $\alpha = \sup_{\rho \in [0,1]} f''(\rho)$.

The proof is postponed to Appendix A.

Main ideas of the proof of Theorem 1.
Let an unknown initial data $\bar{\rho}_0$. For every time $t > 0$, the i-th AV (denoted by AV_i) measures locally in time the density $\rho(t, y_i(t)\pm)$ and its new speed becomes $u_i(\rho(t, y_i(t)+))$. The trajectory of AV_i is described by (3). Since $u_i(\rho) \geqslant f'(\rho)$ for every $\rho \in [0, 1]$, the speed of AV_i is faster than (or equal to) the speed of every discontinuity. At time T_i, defined in (6), the AV_i has already interacted with every discontinuity wave coming from $(0, x)$ with $x \in (y_0^i, y_0^{i+1})$ or from (t, α) with $t \in (t_{i+1}, t_i)$. Thus, the solution over $\{(T_i, x) \in \mathbb{R}_+ \times \mathbb{R} / y_i(T_i) \leqslant x \leqslant y_{i+1}(T_i)\}$ can be deduced using only the data $\rho(\cdot, y_{i+1}(\cdot)-)$ collected by the AV_{i+1}. Therefore, Theorem 1 is proved using the uniqueness of (LWR) defined on $\{(t, x) \in \mathbb{R}_+ \times \mathbb{R}, x < y_{i+1}(t)\}$ with boundary condition $\rho(\cdot, y_{i+1}(\cdot))$.

The assumption in Theorem 1 can be relaxed if the speed of AV_i is constant.

Lemma 1. *Let $i \in \{-N_1, \cdots, N_2\}$. We assume that $u_i(\rho) \geqslant f'(\rho)$. Let $T_i > 0$ such that (6) holds. If there exists $a \in \mathbb{R}_+$ and $b \in \mathbb{R}_+$ such that $\rho(\cdot, y_i(\cdot))$ is a constant function over $[a, b)$ and $T_i \in [a, b)$ then, for every $\rho_0 \in \Gamma^{-1}(\Gamma(\bar{\rho}_0))$, $S_a(\rho_0)(x) = S_a(\bar{\rho}_0)(x)$ for almost every $x \in [y_i(a), y_{i+1}(a)]$ with (y_i, y_{i+1}) solution of (3).*

The proof is deferred to Appendix A.

3.1 Extension to ring roads

We consider a ring of length L. By detecting local traffic density via $M + 1$ autonomous vehicles, we want to reconstruct the whole density on the ring at a certain time $T_{\max}$. Mathematically speaking, the i^{th} autonomous vehicles, where the trajectory $y_i(\cdot)$ is modeled by (3) with $t_i = 0$, detects the local density $\rho(\cdot, y_i(\cdot)\pm)$. From datum $(\rho(\cdot, y_i(\cdot)))_{i\in\{1,\cdots,M\}}$ we want to reconstruct $\rho(T_{\max}, \cdot)$ on the whole ring. We consider the following PDE-ODE system

$$\begin{cases} \partial_t \rho + \partial_x(f(\rho)) = 0, & (t, x) \in \mathbb{R}^+ \times \mathbb{R}, \\ \rho(0, x) = \rho_0(x), & x \in \mathbb{R}, \\ \dot{y}_i^j(t) = u_i(\rho(t, y_i^j(t)+))), & t \in \mathbb{R}^+, i = 0, \cdots, M, \, j \in \mathbb{Z}, \\ y_i^j(0) = y_0^i + jL, & i = 0, \cdots, M, \, j \in \mathbb{Z}, \end{cases} \tag{LWR-AVs-ring}$$

where $\rho_0(\cdot)$ is a L-periodic function. Combining Theorem 1 with Theorem 2, we have the following.

Theorem 3. *We assume that, for every $x \in \mathbb{R}$, $0 < \rho_{\min} \leqslant \bar{\rho}_0(x) \leqslant \rho_{\max}$ and let $c = \min_{i\in\{0,\cdots,M\}} \min_{\rho\in[\rho_{\min},\rho_{\max}]}(u_i(\rho) - f'(\rho))$. There exists a time $T_{max} < \infty$ verifying that*

$$\frac{\min_{i\in\{0,\cdots,M\}}(y_0^{i+1} - y_0^i)}{f'(\rho_{\min}) - f'(\rho_{\max})} < T_{max} < \max_{i\in\{0,\cdots,M\}}(y_0^{i+1} - y_0^i)\left(\frac{1 + \exp(\frac{\alpha TV(\rho_0)}{c})}{c}\right),$$

such that we can reconstruct the whole density on the ring at time t verifying $t \geqslant T_{\max}$ only using datum collected by $M + 1$ autonomous vehicles.

Proof. Instead of considering $\{y_i^j, j \in \mathbb{Z}\}$ as one autonomous vehicle, each element in $\{y_i^j, j \in \mathbb{Z}\}$ is considering as an unique autonomous vehicle. Thus, replacing y_i^j by y_{jM+j+i} in (LWR-AVs-ring), the system (LWR-AVs-ring) is rewritten as

$$\begin{cases} \partial_t \rho + \partial_x(f(\rho)) = 0, & (t,x) \in \mathbb{R}^+ \times \mathbb{R}, \\ \rho(0,x) = \rho_0(x), & x \in \mathbb{R}, \\ \dot{y}_{jM+j+i}(t) = u_{jM+j+i}(\rho(t, y_{jM+j+i}(t)+))), & t \in \mathbb{R}^+, i = 0, \cdots, M \text{ and } j \in \mathbb{Z} \\ y_{jM+j+i}(0) = y^0_{jM+j+i}, & i = 0, \cdots, M \text{ and } j \in \mathbb{Z} \end{cases}$$

Applying Theorem 1 and Theorem 2 with $N_2 = M$ and $N_1 = 0$, the proof is done. □

4 Numerical scheme

The goal of this section is to describe the numerical scheme that is used to reconstruct the density. Our aim is to design a scheme that is able to approximate numerically on a fixed mesh the conservation law and the autonomous vehicles and use this scheme for the reconstruction algorithm. In the following section we show how to simulate the PDE-ODE system by describing the numerical methods adopted and then we describe in detail the reconstruction algorithm.

4.1 Construction of the true state (ρ^n, y^n)

4.1.1 Wave-front tracking method for the conservation law

To construct piecewise constant approximate solutions, we adapt the standard wave front tracking method, see for example [4, Chapter 6]. The goal of the Wave-Front Tracking (WFT) method is to approximate and compute the solution of the conservation law. Fix a positive $n \in \mathbb{N}$, $n > 0$ and introduce in $[0,1]$ the mesh $\mathcal{M}_n = \{\rho_i^n\}_{i=0}^{2^n}$ defined by

$$\mathcal{M}_n = (2^{-n}\mathbb{N} \cap [0,1]).$$

The WFT method works as follows:

1) Approximate the initial data $\rho_0 \in \mathrm{BV}(\mathbb{R}, [0,1])$ with piecewise constant functions $\rho_0^n \in \mathcal{M}_n$.

2) Solve the Riemann problems generated by the jumps $(\rho_0^n(x_i-), \rho_0^n(x_i+))$ for $i = 1, \cdots, N$ where $x_0 < \cdots < x_N$ are the points where ρ_0^n is discontinuous.

3) Piece the solutions together approximating rarefaction waves with fans of rarefaction shocks where the speed of each one has strength 2^{-n} and is prescribed by the Rankine-Hugoniot condition.

4) The piecewise constant approximate solution ρ^n constructed can be prolonged up to the fist time $t_1 > 0$, where two discontinuities collide. In this case, a new Riemann problem arises and needs to be solved.

4.1.2 Numerical method for the ODE

Let $\rho^n(t,\cdot)$ the WFT approximate solution associated to ρ_0^n (see Subsection 4.1.1). We describe in this section how to solve numerically the following ODE

$$\begin{cases} \dot{y}_i^n(t) = u_i(\rho^n(t, y_i^n(t)+)) & t \in [t_i, +\infty], i = -N_1, \cdots, N_2, \\ y(t_i) = y_0^i & i = -N_1, \cdots, N_2. \end{cases} \tag{8}$$

. Since the solution y_i^n of (8) is a piecewise constant function, it is enough to find the points of discontinuity of y_i^n, denoted by $(t_{i,k}, y_i^{n,k})_{k\in\{1,\cdots,K\}}$.

Step 0. We impose $(t_{i,0}, y_i^{n,0}) = (t_i, y_0^i)$.
Step 1. From $(t_{i,k}, y_i^{n,k})$, we determine the position of the autonomous vehicles $(t_{i,k+1}, y_i^{n,k+1})$ as follows. For the ODE (8), we have

$$y_i^{n,k+1} = u_i(\rho^n(t_{i,k}, y_i^{n,k}+)))(t_{i,k+1} - t_{i,k}) + y_i^{n,k}$$

and $t_{i,k+1}$ is the first interaction time between the straight line defined by

$$\{u_i(\rho^n(t, y_i^{n,k}+)))(t - t_{i,k}) + y_i^{n,k}, t > t_{i,k}\}$$

and elements of the set of discontinuity waves of $\rho^n(t,\cdot)$ with $t > t_{i,k}$.

4.2 Reconstruction scheme

In this section we describe in detail the algorithm for the density reconstruction which is composed by the following steps, for simplicity we drop the index n. We assume that the initial density $\rho_0 \in \mathcal{M}_n$ is a piecewise constant function and ρ is the solution of (LWR) with initial density ρ_0.
Algorithm. Algorithm for the reconstruction of the density between two AVs i and $i+1$.

Input data:

- Discontinuity points $(t_{i,k})_{k\in\{1,\cdots,K\}}$ of y_i
- AV trajectories: $y_i(t_{i,k}) := y_i^k$ and $y_{i+1}(t_{i,k}) := y_{i+1}^k$.
- Densities measured by the AV $\rho(t_{i,k}, y_i^k\pm))$ and $\rho(t_{i,k}, y_{i+1}^k\pm))$.

Step 0. Impose $t_{i,K+1} = \infty$, $\rho_{i+1,\text{rec}}(t,x) = \rho(t_{i+1}, y_0^{i+1}-)$ for every $(t,x) \in [t_{i+1}, t_{i+1,1}] \times \mathbb{R}$. To avoid misunderstanding, we recall that t_{i+1} is the starting time of AV_i and $t_{i+1,1} > t_{i+1}$ is the first discontinuity point of y_i.

Step 1. Compute the reconstruction density $\rho_{i+1,\text{rec}}(t_{i+1,k},\cdot)$ at every time $t_{i+1,k}$ only using data collected by the $(i+1)^{\text{th}}$-autonomous vehicle.
For every $k \in \{1,\cdots,K-1\}$,

- Solve all the Riemann problem at time $t_{i+1,k}$ for (LWR-AVs) associated with

$$\rho_{i+1,\text{rec}}(t_{i+1,k},\cdot)\mathbb{1}_{(\infty,y_{i+1}(t_{i+1,k}))} + \rho(t_{i+1,k},y_{i+1}(t_{i+1,k}+))\mathbb{1}_{(y_{i+1}(t_{i+1,k}),\infty)}.$$

- Piece solutions together where the speed of each wave front is prescribed by the Rankine-Hugoniot condition.

- The solution still denoted by $\rho_{i+1,\text{rec}}$, is prolonged until $\min(t_1, t_{i+1,k+1})$ where t_1 is the first time when two wave-fronts interact. If $t_1 \leqslant t_{i+1,k+1}$, the Riemann problems associated to $\rho_{i+1,\text{rec}}(t_1,\cdot)$, which is still a piecewise constant function, can again be approximately solved within the class of piecewise constant functions and so on until $t = t_{i+1,k+1}$.

end
We end our construction by taking the restriction over $\{(t,x) \in \mathbb{R}_+ \times [y_i(t), y_{i+1}(t)]\}$.

Step 2. Compute the reconstruction time T_i only using $(y_i^k, \rho(\cdot, y_i^k(\cdot)\pm))$ and y_0^{i+1}.
For every $k \in \{1,\cdots,K\}$,
if $y_0^{i+1} \in [f'(\rho(t,y_i^k-))(t_i - t_{i,k}) + y_i^k, f'(\rho(t,y_i^{k+1}-))(t_i - t_{i,k+1}) + y_i^{k+1}]$ then $T_i = t_{i,k}$.
end

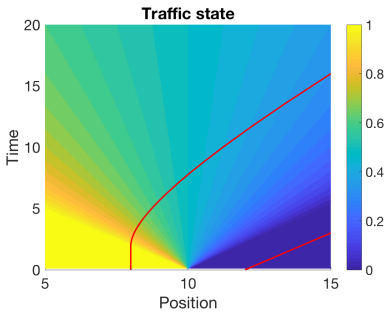
Output data: $\rho_{i+1,\text{rec}}(T_i,x)$, for every $x \in [y_i(T_i), y_{i+1}(T_i)]$

5 Numerical results

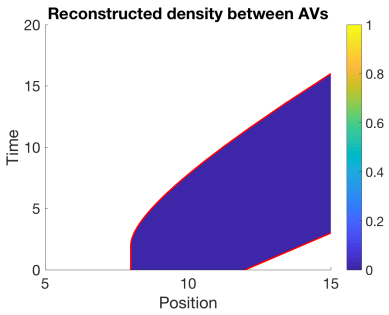
Numerical results are simulated using the flux function $f(\rho) = \rho(1-\rho)$ and the speed of each AV_i is $u_i(\rho) = 1-\rho$. Simulations are conducted using the WFT method described above. Rarefaction shocks are approximated as waves with a change in density of 2^{-5}. This prescribes 33 possible initial densities.

In Figure 3a, we consider the case where the initial density is defined as follows; $\rho_0(x) = 0.9688$ for $x \in (-\infty, 10)$ and $\rho_0(x) = 0.0938$ for $x \in (10,\infty]$ and two autonomous vehicles, denoted by AV_0 and AV_1, are respectively deployed on the road at $(0,8)$ and $(0,12)$ ($N_1 = 0$, $N_2 = 1$ and $N = 2$). The solution (ρ, y_0, y_1) of (LWR-AVs) is

$$\rho(t,x) = \begin{cases} 0.9688 & \text{if } x \leqslant -0.9376t + 10, \\ \frac{1}{2} - (\frac{x-10}{2t}) & \text{if } -0.9376t + 10 \leqslant x \leqslant 0.8124t + 10, \\ 0.0938 & \text{if } 0.8124t + 10 \leqslant x, \end{cases}$$



(a) True state over first 20 seconds solved using wave front tracking.



(b) Reconstructed traffic state using two AVs over first 20 seconds.

Figure 3: Traffic state reconstruction with two autonomous vehicles starting at $x = 8$ and $x = 12$ with initial density defined as follows; $\rho_0(x) = 0.9688$ for $x \in (-\infty, 10)$ and $\rho_0(x) = 0.0938$ for $x \in (10, \infty]$.

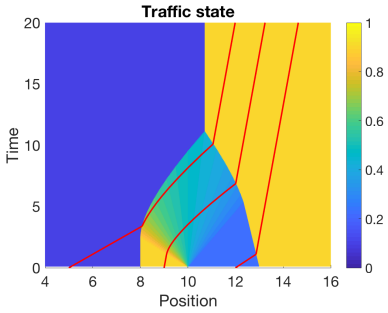
and

$$y_0(t) \approx \begin{cases} 0.0312t + 10 & \text{if } t \leqslant 2.06, \\ 10 + t - 2.78\sqrt{t} & \text{if } 2.06 \leqslant t \leqslant 220.22, \\ 0.9062t - 10.60 & \text{if } 220.22 \leqslant t, \end{cases} \quad \text{and } y_1(t) = 0.9062t + 10.$$

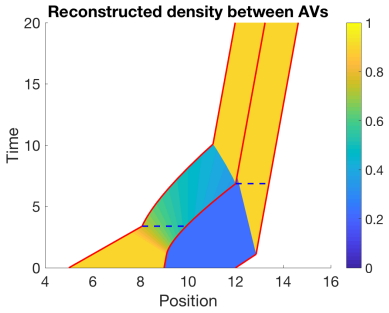
Via sensors of autonomous vehicles, we observe $\rho(\cdot, y_0(\cdot)\pm)$ and $\rho(\cdot, y_1(\cdot)\pm)$. From Theorem 1, $T_0 \approx 240.93$. Using lemma 1, we can reconstruct the density $\rho(220.22, \cdot)$ over $[y_0(220.22), y_1(220.22)]$. To solve numerically (LWR-AVs) with initial density ρ_0, we use the wave-front tracking method described in Subsection 4.1.1 with $n = 5$. The trajectory of autonomous vehicle are plotted in red in Figure 3a and Figure 3b. In Figure 3b, we reconstruct traffic state using two AVs over first 20 seconds. Since we don't observe enough time ($20 < 220.22$), we notice that the reconstructed traffic state is not the true traffic state.

In Figure 4, we consider the example of two shocks with a fan of rarefaction shocks between the two shocks. A total of three AVs, denoted by AV_0, AV_1 and AV_2, are used to reconstruct the traffic state (two regions of reconstruction between AV_0 and AV_1, and between AV_1 and AV_2). Specifically, the initial density ρ_0 is defined as follows; $\rho_0(x) = 0.0938$ for $x \in (-\infty, 8]$, $\rho_0(x) = 0.9062$ for $x \in (8, 10]$, $\rho_0(x) = 0.2188$ for $x \in (10, 13]$ and $\rho_0(x) = 0.9062$ for $x \in (13, \infty)$. AV_0, AV_1, and AV_2 start respectively at $x = 5$, $x = 9$, and $x = 12$. The resulting traffic state solved using wave front tracking over the first 20 seconds in seen in Figure 4a, while the reconstructed state between the AVs is seen in Figure 4b. The time at which the reconstruction becomes valid is $T_0 = 6.87$ between AV_0 an AV_1 and $T_1 = 3.39$ between AV_1 and AV_2.

In Figure 5, a total of four AVs, denoted by AV_0, AV_1, AV_2 and AV_3, are used to reconstruct the traffic state ($N_1 = 0$, $N_2 = 1$ and $N = 2$). The initial density ρ_0 is defined as follows; $\rho_0(x) = 0.0938$ for $x \in (-\infty, 2.1)$, $\rho_0(x) = 0.9688$ for $x \in [2.1, 10.1)$, $\rho_0(x) = 0.2500$ for $x \in [10.1, 12)$, $\rho_0(x) = 0.4375$ for $x \in [12, 16)$,



(a) True state over first 20 seconds solved using wave front tracking.



(b) Reconstructed traffic state using three AVs over first 20 seconds.

Figure 4: Example comparison of true state solved using wave front tracking and the reconstructed state reconstructed using three AVs starting at $x = 5$, $x = 9$ and $x = 12$. The initial density ρ_0 is defined as follows; $\rho_0(x) = 0.0938$ for $x \in (-\infty, 8]$, $\rho_0(x) = 0.9062$ for $x \in (8, 10]$, $\rho_0(x) = 0.2188$ for $x \in (10, 13]$ and $\rho_0(x) = 0.9062$ for $x \in (13, \infty)$.

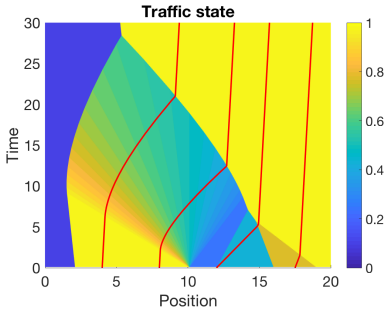
$\rho_0(x) = 0.7812$ for $x \in [16, 19)$, and $\rho_0(x) = 0.9688$ for $x \in [19, \infty)$. The initial positions of AV_0, AV_1, AV_2, and AV_3 are respectively 4, 8, 12 and 17,5. The time at which a reconstruction is found is $T_0 = 5.12$ between AV_0 and AV_1, $T_1 = 12.45$ between AV_1 and AV_2, and $T_2 = 0.00$ between AV_2 and AV_3.

In Figure 6, AV_{-2}, AV_{-1} and AV_0 starts respectively at $(t_{-2}, y_0^{-2}) = (6, 0)$, $(t_{-1}, y_0^{-1}) = (1, 0)$ and $(t_0, y_0^0) = (0, 8)$ ($N_1 = 2$, $N_2 = 0$,$N = 3$). The initial density ρ_0 is defined as follows; $\rho_0(x) = 0.3125$ for $x \in (-\infty, -1]$, $\rho_0(x) = 0.5$ for $x \in [-1, 4]$, $\rho_0(x) = 0.8125$ for $x \in [4, 10]$, and $\rho_0(x) = 0.5$ for $x \in (10, \infty)$. Thus, AV_{-2} and AV_{-1} start after AV_0 is already driving. The times at which the state can be reconstructed is $T_{-2} = 8.615$ for the state between AV_{-2} and AV_{-1}, and $T_{-1} = 5.538$ between the AV_{-1} and AV_0.

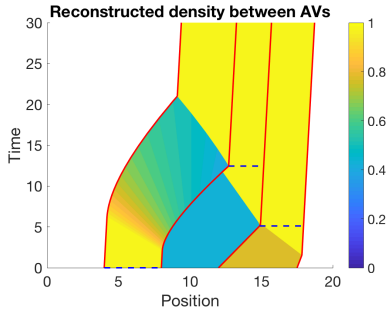
In Figure 7, one autonomous vehicle, denoted by AV_0, is deployed on a ring ($M = 1$ in subsection 3.1). The initial density ρ_0 is a 10-periodic function defined as follows: $\rho_0(x) = 0.8125$ for $x \in (0, 2)$, $\rho_0(x) = 0.3125$ for $x \in (2, 10)$. Since ρ and y_0 are also 10 periodic functions, both trajectories plotted in red in Figure 7b are the ones of AV_0. The whole traffic state on the ring can be reconstructed after $T_{\max} = 15.444$.

6 Conclusions

The main result of this work is the theoretical analysis and a numerical scheme to reconstruct the bulk traffic density using only data along the trajectory of a small number of autonomous vehicles. The results are derived for the case when the bulk flow is described by LWR-type traffic flow models. Moving forward, there are several interesting extensions of the present work. For exam-

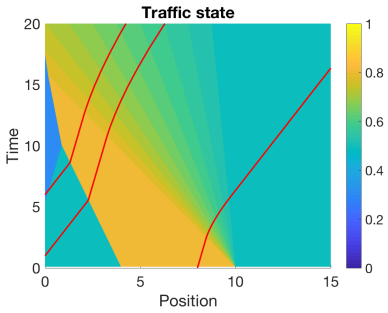


(a) True state over first 30 seconds solved using wave front tracking.

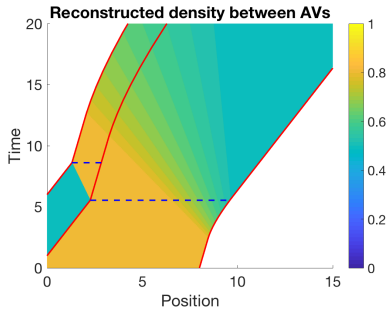


(b) Reconstructed traffic state using four AVs over first 30 seconds.

Figure 5: Example comparison of true state solved using wave front tracking and the reconstructed state reconstructed using four AVs starting at $x = 4, 8, 12$ and $x = 17.5$.

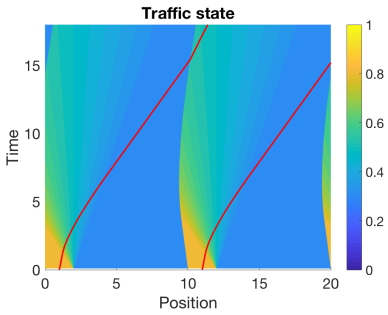


(a) True state over first 20 seconds solved using wave front tracking.

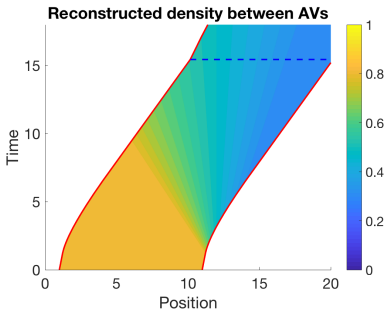


(b) Reconstructed traffic state using two AVs over first 20 seconds.

Figure 6: Traffic state reconstruction with three autonomous vehicles starting at $(t_{-2}, y_0^{-2}) = (6, 0)$, $(t_{-1}, y_0^{-1}) = (1, 0)$ and $(t_0, y_0^0) = (0, 8)$. The initial density ρ_0 is defined as follows; $\rho_0(x) = 0.3125$ for $x \in (-\infty, -1]$, $\rho_0(x) = 0.5$ for $x \in [-1, 4]$, $\rho_0(x) = 0.8125$ for $x \in [4, 10]$, and $\rho_0(x) = 0.5$ for $x \in (10, \infty)$.



(a) True state over first 18 seconds solved using wave front tracking.



(b) Reconstructed traffic state using one AV over first 18 seconds.

Figure 7: Traffic state reconstruction with one autonomous vehicles on a ring of length 10 with a 10-periodic initial density defined as follows; $\rho_0(x) = 0.8125$ for $x \in (0, 2)$, $\rho_0(x) = 0.3125$ for $x \in (2, 10)$.

.

ple, we are interested in also using AVs to estimate the traffic in and around phantom traffic jams [24], which are jams that seemingly appear without a cause but are due to human driving behavior. These jams are particularly challenging to track on real freeways due to the space and timescales on which they are found. Extending the methods developed in the present article to bulk flow models (e.g., [12]) that are able to reproduce these waves is a promising direction. Other directions include extension of the developed methods to traffic flow networks and testing of the algorithm on empirical traffic data collected from the field.

A Proof of Theorem 1, Theorem 2 and Lemma 1

In order to simplify the notations, we introduce the function $g_i : \mathbb{R} \to [0, 1]$ in

$$g_i(t+) := \lim_{x \to y_i(t), y_i(t) < x} \rho(t, x) = \rho(t, y_i(t)+)$$

and

$$g_i(t-) := \lim_{x \to y_i(t), x < y_i(t)} \rho(t, x) = \rho(\cdot, y_i(\cdot)-),$$

where $(\rho(t, y_i(t)\pm))_{i \in \{-N_1, \cdots, N_2\}} = \Gamma(\bar{\rho}_0)$. Since the speed of AVs is faster than (or equal to) the speed of every discontinuity, the function g_i is well-defined.

We recall that the i^{th} autonomous vehicle starts at time t_i in the position y_0^i. If $i \in \{-N_1, \cdots, -1\}$, $y_i^0 = \alpha$ and $t_i > 0$ and if $i \in \{0, \cdots, N_2\}$, $\alpha \leqslant y_i^0$ and $t_i = 0$.

A.1 Generalized characteristics

The proof of Theorem 1, Theorem 2 and Lemma 1 are based on the concept of generalized characteristic (see [7, Chapter XI]). A generalized characteristic $\xi(\cdot)$ is a Lipschitz curve, defined on the time interval $[\sigma,\tau]\subset[0,\infty)$ associated with the solution ρ, verifying for almost $t\in[\sigma,\tau]$,

$$\dot{\xi}(t)=\begin{cases} f'(\rho(t,\xi(t))) & \text{when } \rho(t,\xi(t)+)=\rho(t,\xi(t)-)=\rho(t,\xi(t)),\\ \frac{f(\rho(t,\xi(t)+))-f(\rho(t,\xi(t)-))}{\rho(t,\xi(t)+)-\rho(t,\xi(t)-)} & \text{when } \rho(t,\xi(t)-)<\rho(t,\xi(t)+).\end{cases} \tag{9}$$

Let $\bar{t}>0$. We denote by $\xi_-(\cdot,\bar{t},\bar{x})$ and $\xi_+(\cdot,\bar{t},\bar{x})$ the minimal and maximal backward characteristics, associated with and admissible solutions ρ, coming from a point $(\bar{t},\bar{x})$. From [7, Thm 10.3.1, Thm 11.1.3], we have, for every $i\in\{-N_1,\cdots,N_2\}$,

$$\begin{cases} \xi_-(t,\bar{t},y_i(\bar{t}))=\xi_+(t,\bar{t},y_i(\bar{t}))=f'(g_i(\bar{t}))(t-\bar{t})+y_i(\bar{t}) & \text{when } g_i(\bar{t}-)=g_i(\bar{t}+)\\ \left.\begin{aligned}\xi_-(t,\bar{t},y_i(\bar{t}))&=f'(g_i(\bar{t}-))(t-\bar{t})+y_i(\bar{t})\\ \xi_+(t,\bar{t},y_i(\bar{t}))&=f'(g_i(\bar{t}+))(t-\bar{t})+y_i(\bar{t})\end{aligned}\right| & \text{when } g_i(\bar{t}-)<g_i(\bar{t}+)\end{cases} \tag{10}$$

The next Lemma gives the domain of dependence of (LWR) for a point $(t,x)\in\mathbb{R}_+\times\mathbb{R}$ (see [7, Theorem 10.2.2]).

Lemma 2. *Let $i\in\{-N_1,\cdots,N_2\}$, $\rho_0\in L^1(\mathbb{R})\cap BV(\mathbb{R},[0,1])$ and $(t,x)\in(t_i,\infty)\times[\alpha,\infty)$. The value $S_t(\rho_0)(x):=\rho(t,x)$ depends only on values of $\rho(\cdot,\cdot)$ in the subset $\{(s,y)\in[0,t]\times\mathbb{R}/\xi_-(s,t,x)\leqslant y\leqslant\xi_+(s,t,x)\}\cap\{(s,y)\in[0,t]\times\mathbb{R}/\ y_0^i\leqslant y\}$ of $\mathbb{R}^2$.*

A.2 Some properties of φ_i

First of all, using (10), φ_i defined in (5) can be rewritten as follows;

$$\varphi_i: t\to=[\xi_-(t_{i+1},t,y_i(t)),\xi_+(t_{i+1},t,y_i(t))]. \tag{11}$$

Lemma 3. *φ_i is an increasing application over $[t_{i+1},\infty]$ in the following sense: for every $t_{i+1}\leqslant t_1<t_2$,*

$$f'(g_i(t_1+))(t_{i+1}-t_1)+y_i(t_1)\leqslant f'(g_i(t_2-))(t_{i+1}-t_2)+y_i(t_2).$$

Proof. Let $t_{i+1}\leqslant t_1<t_2$. If $\xi_+(\cdot,t_1,y_i(t_1))$ and $\xi_-(\cdot,t_2,y_i(t_2))$ coincide over $[t_{i+1},t_1]$ then, from (10),

$$f'(g_i(t_1+))(t_{i+1}-t_1)+y_i(t_1)=f'(g_i(t_2-))(t_{i+1}-t_2)+y_i(t_2).$$

Otherwise, since $\xi_+(\cdot,t_1,y_i(t_1))$ and $\xi_-(\cdot,t_2,y_i(t_2))$ are shock-free [1], from [7, Corollary 11.1.2], $\xi_+(\cdot,t_1,y_i(t_1))$ and $\xi_-(\cdot,t_2,y_i(t_2))$ cannot interact for any $t\in(0,t_1]$. Moreover, using that $u_i(\rho)\geqslant f'(\rho)$ for every $\rho\in[0,1]$, we have

[1] A generalized characteristic $\xi(\cdot)$, associated with ρ and defined on $[\sigma,\tau]$, is called shock-free if $\rho(\xi(t)-,t)=\rho(\xi(t)+,t)$, for almost all t in $[\sigma,\tau]$.

$\xi_+(t,t_1,y_i(t_1)) \leqslant \xi_-(t,t_2,y_i(t_2))$ for every $t \in [t_{i+1},t_1]$. In particular, we obtain $\xi_+(t_{i+1},t_1,y_i(t_1)) \leqslant \xi_-(t_{i+1},t_2,y_i(t_2))$. From (10), we deduce that if $t_{i+1} \leqslant t_1 < t_2$ then
$f'(g_i(t_1+))(t_{i+1}-t_1)+y_i(t_1) \leqslant f'(g_i(t_2-))(t_{i+1}-t_2)+y_i(t_2)$.

□

Lemma 4. *Let $0 < \rho_{\min} \leqslant \bar{\rho}_0(\cdot) \leqslant \rho_{\max}$ and $c_i := \min_{\rho\in[\rho_{\min},\rho_{\max}]}(u_i(\rho) - f'(\rho)) > 0$.*

- *Let $t_0 > 0$. Assuming that $g_i'(\cdot)$ is well-defined over (t_0,t_1) and $g_i'(t) < 0$ for every $t \in (t_0,t_1)$ then*

$$t_1 \leqslant t_0 \exp\left(\frac{f'(g_i(t_1-)) - f'(g_i(t_0+))}{c_i}\right). \tag{12}$$

- *Assuming that $g_i(\cdot)$ is an increasing function over (t_0,t_1) then, for every $x_1 \in \varphi_i(t_1)$ and $x_0 \in \varphi_i(t_0)$,*

$$x_1 - x_0 \geqslant c_i(t_1-t_0).$$

- *if $g_i(t_0-) < g_i(t_0+)$ then*

$$\lambda(\varphi_i(t_0)) = (f'(g_i(t_0+)) - f'(g_i(t_0-)))(t_{i+1}-t_0),$$

where λ denotes the Lebesgue measure.

Proof. • Since $g_i'(t) < 0$ for every $t \in (t_0,t_1)$, then there exists $x_r \in R$ such that $g_i(t) = (f')^{-1}(\frac{y_1(t)-x_r}{t})$ for every $t \in (t_0,t_1)$. Thus, y_i verifies

$$\begin{cases} \dot{y}_i(t) = u_i((f')^{-1}(\frac{y_1(t)-x_r}{t})), & t_0 < t \leqslant t_1, \\ y_i(t_0) = x_0. \end{cases}$$

Above, x_r is the starting point of the rarefaction wave crossed by the i^{th} autonomous vehicle over (t_0,t_1). Let $\tilde{y}_i(\cdot)$ defined by

$$\begin{cases} \dot{\tilde{y}}_i(t) = \frac{\tilde{y}_i(t)-x_r}{t} + c_i, & t > t_0, \\ \tilde{y}_i(t_0) = x_0. \end{cases} \tag{13}$$

Since $u_i(\rho) \geqslant f'(\rho) + c_i$, we have $\tilde{y}_i(t) \leqslant y_i(t)$ for every $t \in [t_0,t_1]$. In particular, $\tilde{y}_i(t_1) \leqslant y_i(t_1) = f'(g_i(t_1-))t_1 + x_r$. From (13), for every $t \geqslant t_0$, $\tilde{y}_i(t) = c_i t \ln(\frac{t}{t_0}) + x_r + t f'(g_1(t_0+))$. Thus, we have

$$t_1 \leqslant t_0 \exp\left(\frac{f'(g_i(t_1-)) - f'(g_i(t_0+))}{c_i}\right),$$

whence the conclusion of (12).

- Let $x_1 \in \varphi_i(t_1)$ and $x_0 \in \varphi_i(t_0)$. By definition of φ_i in (5) and using that y_i is solution of (3), we have

$$\begin{array}{rcl} x_1 - x_0 & \geqslant & f'(g_i(t_1-))(t_{i+1}-t_1) + y_i(t_1) - f'(g_i(t_0+))(t_{i+1}-t_0) - y_i(t_0), \\ & \geqslant & f'(g_i(t_1-))(t_{i+1}-t_1) - f'(g_i(t_0+))(t_{i+1}-t_0) + \int_{t_0}^{t_1} u_i(g_i(s))\,ds \end{array}$$

  Since $g_i(\cdot)$ is an increasing function over (t_0, t_1) and $u_i(\rho) \geqslant f'(\rho) + c_i$ for every $\rho \in [\rho_{\min}, \rho_{\max}]$,

$$\begin{array}{rcl} x_1 - x_0 & \geqslant & f'(g_i(t_1-))(t_{i+1}-t_1) - f'(g_i(t_0+))(t_{i+1}-t_0) \\ & & +f'(g_i(t_1-))(t_1-t_0) + c_i(t_1-t_0) \\ & \geqslant & (f'(g_i(t_1-)) - f'(g_i(t_0+)))(t_{i+1}-t_0) + c_i(t_1-t_0) \end{array}$$

  Using that $f'(g_i(t_1-)) - f'(g_i(t_0+)) \leqslant 0$ and $t_{i+1} - t_0 \leqslant 0$, we conclude that

$$x_1 - x_0 \geqslant c_i(t_1 - t_0).$$

- We have

$$\begin{array}{rcl} \lambda(\varphi_i(t_0)) & = & f'(g_i(t_0+))(t_{i+1}-t_0) + y_i(t_0) - f'(g_i(t_0-))(t_{i+1}-t_0) \\ & & +y_i(t_0) \\ & = & (f'(g_i(t_0+)) - f'(g_i(t_0-)))(t_{i+1}-t_0) \end{array}$$

□

A.3 Proof of Theorem 1

Let $\rho_0 \in L^1(\mathbb{R}) \times BV(\mathbb{R}, [0,1])$, $i \in \{-N_1, \cdots, N_2 - 1\}$ and $x \in (y_i(T_i), y_{i+1}(T_i))$.

Since T_i verifies (6) and using that $T_i < +\infty$ with (10), we have

$$y_0^{i+1} \in [\xi_-(t_{i+1}, T_i, y(T_i)), \xi_+(t_{i+1}, T_i, y(T_i))]. \tag{14}$$

Above, $\xi_-(\cdot, T_i, y(T_i))$ and $\xi_+(\cdot, T_i, y(T_i))$ are the minimal and maximal backward characteristics respectively, associated with ρ_0, coming from the point $(T_i, y(T_i))$. Using that $y_i(T_i) < x$ and since T_i verifies (6) we have

$$\xi_+(t_{i+1}, T_i, y(T_i)) < \xi_+(t_{i+1}, T_i, x) \tag{15}$$

From (14) and (15), we conclude that $y_0^{i+1} < \xi_-(t_{i+1}, T_i, x)$. and since $u_{i+1}(\rho) \geqslant f'(\rho)$, $\xi_-(\cdot, T_i, x)$ (resp. $\xi_+(\cdot, T_i, x)$) interacts only once at time $t_- \geqslant t_{i+1}$ (resp. at time $t_+ \geqslant t_{i+1}$) with $y_{i+1}(\cdot)$. Thus, $S_{T_i}(\rho_0)(x)$ depends only on $\{S_t(\rho_0)(y_{i+1}(t)), t \in [t_-, t_+]\}$. Since, for every $\rho_0 \in \Gamma^{-1}(\Gamma(\bar{\rho}_0))$ and for every $t \in \mathbb{R}_+$, $S_t(\rho_0)(y_{i+1}(t)) = S_t(\bar{\rho}_0)(y_{i+1}(t))$, we have

$$S_{T_i}(\rho_0)(x) = S_{T_i}(\bar{\rho}_0)(x).$$

A.4 Proof of Theorem 2

Since, for every $x \in \mathbb{R}$, $0 < \rho_{\min} \leqslant \bar{\rho}_0(x) \leqslant \rho_{\max}$, we have $\rho_{\min} \leqslant g_i(t) \leqslant \rho_{\max}$ for every $i \in \{-N_1, \cdots, N_2\}$. Thus, for every $t \geqslant t_{i+1}$,

$$\varphi_i(t) \subset [(t-t_{i+1})(u_i(\rho_{\max}) - f'(\rho_{\min})) + y_0^i, (t-t_{i+1})(u_i(\rho_{\min}) - f'(\rho_{\max})) + y_0^i].$$

Since $u_i(\rho) \geqslant f'(\rho)$, for every $\rho \in [0,1]$, we have $u_i(\rho_{\min}) - f'(\rho_{\max}) \geqslant 0$ and we conclude that

$$T_i \geqslant \frac{y_0^{i+1} - y_0^i}{u_i(\rho_{\min}) - f'(\rho_{\max})} + t_{i+1}.$$

Since the quantity $u_i(\rho_{\max}) - f'(\rho_{\min})$ may be negative, find an upper bound of T_i is not as straightforward as the above. Using $TV(\bar{\rho}_0) < \infty$, there exists $(\bar{t}_{2k+1})_{k\in\{0,\cdots,N\}}$ such that $g_i(\cdot)$ is a non-increasing function over $\cup_{k=0}^{N}(\bar{t}_{2k+1}, \bar{t}_{2k+2})$ with $N \in \mathbb{N}\cup\{\infty\}$ and $g_i(\cdot)$ is an increasing function over $\mathbb{R}\backslash\{\cup_{k=0}^{N}(\bar{t}_{2k+1}, \bar{t}_{2k+2})\}$. For every $k \in \{0, \cdots, N\}$, $\bar{t}_{2k+1} \geqslant t_{i+1}$ and since y_i is solution of (3), we have $\bar{t}_1 > 0$. We introduce the set $\mathcal{I} \subset \mathbb{N} \cup \{\infty\}$ defined by

$$\mathcal{I} = \left\{k \in \mathbb{N}\cup\{\infty\} / \xi_+(t_{i+1}, \bar{t}_{2k+1}, y_i(\bar{t}_{2k+1})) = \xi_-(t_{i+1}, \bar{t}_{2k+2}, y_i(\bar{t}_{2k+2})) \leqslant y_0^{i+1}.\right\}$$

Using (12), for every $k \in \mathbb{N}$, we have

$$\begin{cases} \bar{t}_{2k+2} \leqslant \bar{t}_{2k+1} \exp\left(\frac{f'(g_i(\bar{t}_{2k+2}-)) - f'(g_i(\bar{t}_{2k+1}+))}{c_i}\right), \\ \bar{t}_{2k} \leqslant \bar{t}_{2k-1} \exp\left(\frac{f'(g_i(\bar{t}_{2k}-)) - f'(g_i(\bar{t}_{2k-1}+))}{c_i}\right). \end{cases} \tag{16}$$

If $\bar{t}_{2k+1} = \bar{t}_{2k}$, from (16), we have immediately that

$$\bar{t}_{2k+2} \leqslant \bar{t}_{2k-1} \exp\left(\frac{f'(g_i(\bar{t}_{2k+2}-)) - f'(g_i(\bar{t}_{2k+1}+)) + f'(g_i(\bar{t}_{2k}-)) - f'(g_i(\bar{t}_{2k-1}+))}{c_i}\right). \tag{17}$$

Otherwise,

$$\begin{aligned} \bar{t}_{2k+2} \leqslant \quad & \exp\left(\frac{f'(g_i(\bar{t}_{2k+2}-)) - f'(g_i(\bar{t}_{2k+1}+))}{c_i}\right) \\ & \left(\bar{t}_{2k+1} - \bar{t}_{2k} + \bar{t}_{2k-1} \exp\left(\frac{f'(g_i(\bar{t}_{2k}-)) - f'(g_i(\bar{t}_{2k-1}+))}{c_i}\right)\right). \end{aligned} \tag{18}$$

Since, for every $k \in \mathbb{N}$,
$f'(g_i(\bar{t}_{2k+2}-)) - f'(g_i(\bar{t}_{2k+1}+) \leqslant \alpha(g_i(\bar{t}_{2k+1}+) - g_i(\bar{t}_{2k+2}-))$ with
$\alpha = \sup_{\rho\in[\rho_{\min},\rho_{\max}]} f''(\rho)$, we have, for every $p \in \{0, \cdots, k\}$,

$$\sum_{j=p}^{k} \frac{f'(g_i(\bar{t}_{2j+2}-)) - f'(g_i(\bar{t}_{2j+1}+))}{c_i} \leqslant \frac{\alpha TV(\bar{\rho}_0)}{c_i}. \tag{19}$$

We introduce $A(k) = \{j \in \{0, \cdots, k\} / \bar{t}_{2j+1} \neq \bar{t}_{2j}\}$. Using (17), (18) and (19), by induction we obtain, for every $k \in \mathbb{N}$,

$$\bar{t}_{2k+2} \leqslant \left(\sum_{j \in A(k)} (\bar{t}_{2j+1} - \bar{t}_{2j}) \right) \exp\left(\frac{\alpha TV(\bar{\rho}_0)}{c_i} \right). \tag{20}$$

Above, $\bar{t}_0 := 0$, $\bar{t}_1 \geqslant t_{i+1}$ and $\bar{t}_1 > 0$.

- If $t_i = 0$; we have immediately that $t_{i+1} = 0$. For every $j \in A(k)$, for every $t \in (\bar{t}_{2j}, \bar{t}_{2j+1})$, $g_i(\cdot)$ is an increasing function, using 4, we have, for every $x_{2j} \in \varphi_i(\bar{t}_{2j})$ and for every $x_{2j+1} \in \varphi_i(\bar{t}_{2j+1})$,

$$x_{2j+1} - x_{2j} \geqslant c_i(\bar{t}_{2j+1} - \bar{t}_{2j}). \tag{21}$$

  Since $\bar{t}_1 > 0$ and $\bar{t}_0 := 0$, we have $0 \in A(k)$ and $\varphi_i(0+) = \{y_0^i\}$. Since $k \in \mathcal{I}$, for every $x_{2k+1} \in \varphi(\bar{t}_{2k+1})$, $x_{2k+1} \leqslant y_0^{i+1}$. Using that, by 3, φ_i is an increasing function and (21), we conclude that

$$\sum_{j \in A(k)} (\bar{t}_{2j+1} - \bar{t}_{2j}) \leqslant \frac{y_0^{i+1} - y_0^i}{c_i}. \tag{22}$$

- If $t_i \neq 0$; by definition of φ_i in (5) and using that $0 < \rho_{\min} \leqslant \bar{\rho}_0(x) \leqslant \rho_{\max}$, for every $x \in \varphi_i(t_i+)$, $x \geqslant f'(\rho_{\min})(t_{i+1} - t_i) + y_0^{i+1}$. Since $k \in \mathcal{I}$, for every $x_{2k+1} \in \varphi(\bar{t}_{2k+1})$, $x_{2k+1} \leqslant y_0^{i+1}$. Using that, by 3, φ_i is an increasing function, we conclude that

$$\sum_{j \in A(k)} (\bar{t}_{2j+1} - \bar{t}_{2j}) \leqslant \frac{y_0^{i+1} - y_0^i + f'(\rho_{\min})(t_i - t_{i+1})}{c_i}. \tag{23}$$

Combining (20) with (23), we have, for every $i \in \mathbb{N}^*$,

$$t_{2k+2} \leqslant \frac{(y_0^{i+1} - y_0^i + f'(\rho_{\min})(t_i - t_{i+1})) \exp(\frac{\alpha TV(\bar{\rho}_0)}{c_i})}{c_i} < +\infty. \tag{24}$$

- If $\mathrm{Card}(\mathcal{I}) < \infty$; we have $T_i \in [t_{2\mathrm{Card}(\mathcal{I})+2}, t_{2\mathrm{Card}(\mathcal{I})+3}]$ and $g_i(\cdot)$ is an increasing function over $(t_{2\mathrm{Card}(\mathcal{I})+2}, t_{2\mathrm{Card}(\mathcal{I})+3})$. We notice that $t_{2\mathrm{Card}(\mathcal{I})+3})$ may be infinite. Thus, from 4, we deduce that

$$T_i - t_{2\mathrm{Card}(\mathcal{I})+2} \leqslant \frac{(y_0^{i+1} - (f'(\rho_{\min})(t_{i+1} - t_i) + y_0^i))}{c_i}.$$

  Using (24), we conclude that

$$T_i \leqslant \frac{(y_0^{i+1} - y_0^i + f'(\rho_{\min})(t_i - t_{i+1}))}{c_i} \left(1 + \exp\left(\frac{\alpha TV(\bar{\rho}_0)}{c_i} \right) \right).$$

- If $\mathrm{Card}(\mathcal{I}) = \infty$; from (24), the increasing sequence $\{t_{2k+2}\}_{k\in\mathcal{I}}$ is bounded. Thus, there exists $t_\infty (\geqslant t_{i+1})$ such that $\lim_{k\to\infty} t_{2k+2} = t_\infty$.
From 4, we deduce that

$$T_i - t_\infty \leqslant \frac{(y_0^{i+1} - y_0^i + f'(\rho_{\min})(t_i - t_{i+1}))}{c_i}.$$

Using (24), we conclude that

$$T_i \leqslant \frac{(y_0^{i+1} - y_0^i + f'(\rho_{\min})(t_i - t_{i+1}))}{c_i}\left(1 + \exp\left(\frac{\alpha TV(\bar{\rho}_0)}{c_i}\right)\right).$$

A.5 Proof of Lemma 1

Let $\rho_0 \in L^1(\mathbb{R})\times BV(\mathbb{R},[0,1])$, $i \in \{-N_1,\cdots,N_2-1\}$ and $x \in (y_i(a), y_{i+1}(a))$. Since $g_i(cdot) := \rho(\cdot, y_i(\cdot)$ is a constant function over $[a,b)$ and $T_i \in [a,b)$ we have, for every $t \in [t_{i+1}, T_i]$,

$$f'(g_i(T_i)-)(t-t_i) + y_i(T_i) = f'(g_i(T_i)+)(t-T_i) + y_i(T_i).$$

By definition of T_i in (6), if $x > f'(g_i(T_i))(a-T_i) + y_i(T_i)$, $S_a(\rho_0)(x)$ only depends on $\{S_t(\rho_0)(y_{i+1}(t), t \in \mathbb{R}\}$. If $y_i(a) \leqslant x \leqslant f'(g_i(T_i))(a-T_i) + y_i(T_i)$, since g_i is a constant function over $[a,b)$ and $u_i(\rho) \geqslant f'(\rho)$ for every $\rho \in [0,1]$, no waves can interact with the straight line passing by $(a, y_i(a))$ and $(T_i, y_i(T_i))$ and therefore with the straight line passing by $(a, y_i(a))$ and $(a, f'(g_i(T_i))(a - T_i) + y_i(T_i))$. We conclude that $S_a(\rho_0)(x)$ depends only on $\{S_t(\rho_0)(y_{i+1}(t)), t \in \mathbb{R}_+\}$. Since, for every $\rho_0 \in \Gamma^{-1}(\Gamma(\bar{\rho}_0))$ and for every $t \in \mathbb{R}_+$, $S_t(\rho_0)(y_{i+1}(t)) = S_t(\bar{\rho}_0)(y_{i+1}(t))$, we have

$$S_a(\rho_0)(x) = S_a(\bar{\rho}_0)(x).$$

Acknowledgments

M.L.D.M. acknowledges the support of the IDEX-IRS 2018 project "MAVIT - Modeling autonomous vehicles in traffic flow" and the support of Inria associated team "MEMENTO".

References

[1] D. Amadori and R. M. Colombo, *Continuous dependence for 2× 2 conservation laws with boundary*, journal of differential equations, 138 (1997), pp. 229–266.

[2] C. Bardos, A.-Y. LeRoux, and J.-C. Nédélec, *First order quasilinear equations with boundary conditions*, Communications in partial differential equations, 4 (1979), pp. 1017–1034.

[3] S. Bianchini and L. V. Spinolo, *The boundary riemann solver coming from the real vanishing viscosity approximation*, Archive for Rational Mechanics and Analysis, 191 (2009), p. 1.

[4] A. Bressan, *Hyperbolic systems of conservation laws*, vol. 20 of Oxford Lecture Series in Mathematics and its Applications, Oxford University Press, Oxford, 2000. The one-dimensional Cauchy problem.

[5] R. M. Colombo and F. Marcellini, *A mixed ode–pde model for vehicular traffic*, Mathematical Methods in the Applied Sciences, 38 (2015), pp. 1292–1302.

[6] R. M. Colombo and A. Marson, *A hölder continuous ode related to traffic flow*, Proceedings of the Royal Society of Edinburgh Section A: Mathematics, 133 (2003), pp. 759–772.

[7] C. M. Dafermos, *Hyperbolic conservation laws in continuum physics, volume 325 of grundlehren der mathematischen wissenschaften [fundamental principles of mathematical sciences]*, 2010.

[8] M. L. Delle Monache and P. Goatin, *Scalar conservation laws with moving constraints arising in traffic flow modeling: an existence result*, Journal of Differential equations, 257 (2014), pp. 4015–4029.

[9] C. Donadello and A. Marson, *Stability of front tracking solutions to the initial and boundary value problem for systems of conservation laws*, Nonlinear Differential Equations and Applications NoDEA, 14 (2007), pp. 569–592.

[10] F. Dubois and P. Le Floch, *Boundary conditions for nonlinear hyperbolic systems of conservation laws*, Journal of Differential Equations, 71 (1988), pp. 93–122.

[11] A. Ferrara, S. Sacone, and S. Siri, *State estimation in freeway traffic systems*, in Freeway Traffic Modelling and Control, Springer, 2018, pp. 169–190.

[12] M. R. Flynn, A. R. Kasimov, J.-C. Nave, R. R. Rosales, and B. Seibold, *Self-sustained nonlinear waves in traffic flow*, Physical Review E, 79 (2009), p. 056113.

[13] M. Fountoulakis, N. Bekiaris-Liberis, C. Roncoli, I. Papamichail, and M. Papageorgiou, *Highway traffic state estimation with mixed connected and conventional vehicles: Microscopic simulation-based testing*, Transportation Research Part C: Emerging Technologies, 78 (2017), pp. 13–33.

[14] D. C. Gazis and C. H. Knapp, *On-line estimation of traffic densities from time-series of flow and speed data*, Transportation Science, 5 (1971), pp. 283–301.

[15] J. C. Herrera and A. M. Bayen, *Incorporation of lagrangian measurements in freeway traffic state estimation*, Transportation Research Part B: Methodological, 44 (2010), pp. 460–481.

[16] J. C. Herrera, D. B. Work, R. Herring, X. J. Ban, Q. Jacobson, and A. M. Bayen, *Evaluation of traffic data obtained via GPS-enabled mobile phones: The Mobile Century field experiment*, Transportation Research Part C: Emerging Technologies, 18 (2010), pp. 568–583.

[17] M. J. Lighthill and G. B. Whitham, *On kinematic waves. ii. a theory of traffic flow on long crowded roads*, Proceedings of the Royal Society of London. Series A, Mathematical and Physical Sciences, 229 (1955), pp. 317–345, http://www.jstor.org/stable/99769.

[18] L. Mihaylova, R. Boel, and A. Hegyi, *Freeway traffic estimation within particle filtering framework*, Automatica, 43 (2007), pp. 290–300.

[19] P. Richards, *Shock waves on the highway*, Operations Research, 4 (1956), pp. 42–51, https://doi.org/10.1287/opre.4.1.42, https://doi.org/10.1287/opre.4.1.42, https://arxiv.org/abs/https://doi.org/10.1287/opre.4.1.42.

[20] T. Seo, A. M. Bayen, T. Kusakabe, and Y. Asakura, *Traffic state estimation on highway: A comprehensive survey*, Annual Reviews in Control, 43 (2017), pp. 128–151.

[21] T. Seo and T. Kusakabe, *Probe vehicle-based traffic state estimation method with spacing information and conservation law*, Transportation Research Part C: Emerging Technologies, 59 (2015), pp. 391 – 403, https://doi.org/https://doi.org/10.1016/j.trc.2015.05.019, http://www.sciencedirect.com/science/article/pii/S0968090X15002132. Special Issue on International Symposium on Transportation and Traffic Theory.

[22] D. Serre, *Systems of Conservation Laws 1: Hyperbolicity, entropies, shock waves*, Cambridge University Press, 1999.

[23] D. Serre, *Systems of conservation laws. 2. geometric structures, oscillations, and initial-boundary value problems. translated from the 1996 french original by in sneddon*, 2000.

[24] Y. Sugiyama, M. Fukui, M. Kikuchi, K. Hasebe, A. Nakayama, K. Nishinari, S.-i. Tadaki, and S. Yukawa, *Traffic jams without bottlenecks - experimental evidence for the physical mechanism of the formation of a jam*, New journal of physics, 10 (2008), p. 033001.

[25] M. W. Szeto and D. C. Gazis, *Application of kalman filtering to the surveillance and control of traffic systems*, Transportation Science, 6 (1972), pp. 419–439.

[26] Y. Wang, M. Papageorgiou, and A. Messmer, *Real-time freeway traffic state estimation based on extended kalman filter: A case study*, Transportation Science, 41 (2007), pp. 167–181.

[27] D. B. Work, S. Blandin, O.-P. Tossavainen, B. Piccoli, and A. M. Bayen, *A traffic model for velocity data assimilation*, Applied Mathematics Research eXpress, 2010 (2010), pp. 1–35.

[28] Y. Yuan, J. Van Lint, R. E. Wilson, F. van Wageningen-Kessels, and S. P. Hoogendoorn, *Real-time lagrangian traffic state estimator for freeways*, IEEE Transactions on Intelligent Transportation Systems, 13 (2012), pp. 59–70.